

Potential Field, Geoelectrical and Reflection Seismic Investigations for Massive Sulphide Exploration in the Skellefte Mining District, Northern Sweden

Saman TAVAKOLI¹, Mahdieh DEGHANNEJAD²,
María de los Ángeles GARCÍA JUANATEY², Tobias E. BAUER¹,
Pär WEIHED¹, and Sten-Åke ELMING¹

¹Division of Geosciences and Environmental Engineering,
Luleå University of Technology, Luleå, Sweden;
e-mail: saman.tavakoli@ltu.se

²Department of Earth Sciences, Division of Geophysics, Uppsala University,
Uppsala, Sweden

Abstract

Multi-scale geophysical studies were conducted in the central Skellefte district (CSD) in order to delineate the geometry of the upper crust (down to maximum ~ 4.5 km depth) for prospecting volcanic massive sulphide (VMS) mineralization. These geophysical investigations include potential field, resistivity/induced polarization (IP), reflection seismic and magnetotelluric (MT) data which were collected between 2009 and 2010. The interpretations were divided in two scales: (i) shallow (~ 1.5 km) and (ii) deep (~ 4.5 km). Physical properties of the rocks, including density, magnetic susceptibility, resistivity and chargeability, were also used to improve interpretations. The study result delineates the geometry of the upper crust in the CSD and new models were suggested based on new and joint geophysical interpretation which can benefit VMS prospecting in the area. The result also indicates that a strongly

conductive zone detected by resistivity/IP data may have been missed using other geophysical data.

Key words: potential field data, seismic reflection, resistivity, induced polarization, magnetotelluric, 3D modeling.

1. INTRODUCTION

The Skellefte mining district (Fig. 1) is regarded as a major ore district in Sweden and one of the main paleoproterozoic arc systems in the world (Weiheid 2010) which produces base metals including Zn, Cu, Pb, Ag, and Au, from VMS and organic gold deposits (Bauer 2010). The economical importance of the district, and international increase in metal price, led to numerous exploration activities in the CSD during recent years (see, *e.g.*, Allen *et al.* 1996, Bauer *et al.* 2011, 2013; Dehghannejad *et al.* 2012a, García Juanatey 2012, Hübert *et al.* 2013, Skyttä *et al.* 2012, Tavakoli *et al.* 2012a, b; Weiheid 2010). To date, nearly 160 million tons of ore is excavated, containing 1.9 ppm gold, 47 ppm silver, 0.7% copper, 0.3% zinc, 0.4% lead, 0.8% arsenic, and 25% sulphur (Kathol and Weiheid 2005).

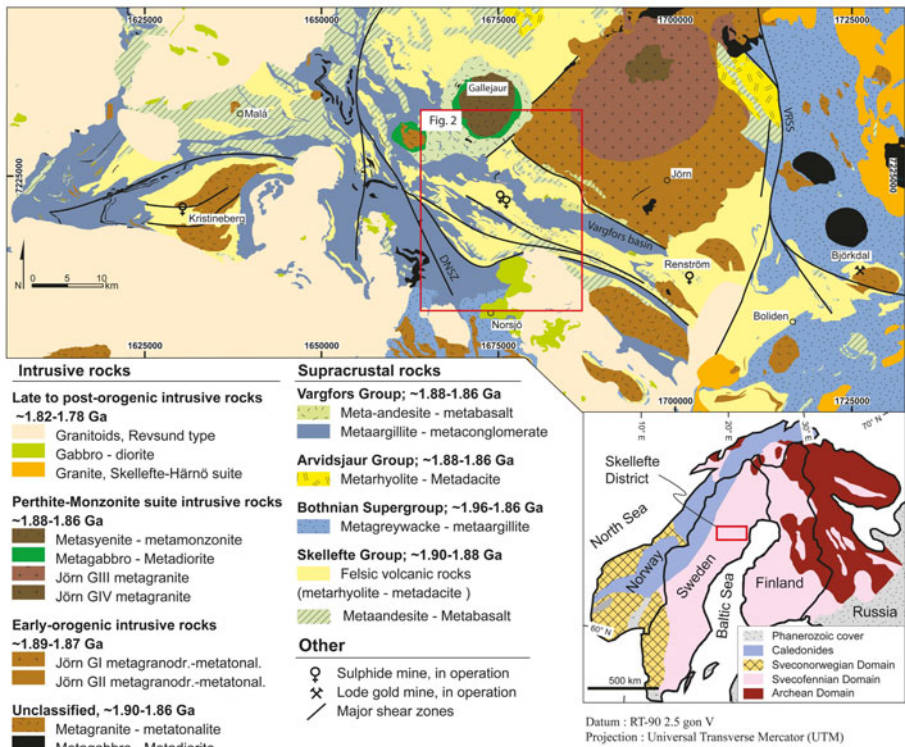


Fig. 1. Overview of the Skellefte district (modified after Kathol and Weiheid 2005).

Exploration activities, including geological and geophysical investigations were initiated in 2008 in the CSD within a framework of the VINNOVA 4D project. These efforts were conducted to expand exploration activities using multiple geological and geophysical studies by modeling the crust in 3D, followed by illustrating the dynamic evolution of the crust through 4D-animation (Skyttä 2012). These geophysical investigations were conducted in the field between 2009 and 2010 (Table 1).

Table 1

Characteristic of the geophysical studies and the measured profiles in the CSD

Geophysical method	Year measured	Item	Profiles									
			I	II	E-1	3D	C1	C2	C3	P1	P2	P3
2009-2D resistivity/IP	2009	i	yes	yes	no	no	no	no	no	yes	yes	–
		ii	5.6	6.8	–	–	–	–	–	27	27	–
		iii	0.43	0.43	–	–	–	–	–	10	10	–
		iv	–	–	–	–	–	–	–	–	–	–
2010-2D resistivity/IP	2010	i	no	no	yes	no	no	no	no	no	no	–
		ii	–	–	10	–	–	–	–	–	–	–
		iii	–	–	1.5	–	–	–	–	–	–	–
		iv	–	–	–	–	–	–	–	–	–	–
3D resistivity/IP	2010	i	no	no	yes	yes	no	no	no	no	–	–
		ii	–	–	1.8	1.8	–	–	–	–	–	–
		iii	–	–	0.5	0.5	–	–	–	–	–	–
		iv	–	–	–	2.16	–	–	–	–	–	–
Magnetic	Various years	i	yes	yes	yes	yes	yes	yes	yes	yes	yes	–
		ii	5.6	6.8	10	–	22.2	21.5	24.45	22.2	21.5	24.45
		iii	0.43	0.43	1.5	–	4.5	4.5	4.5	4.5	4.5	–
		iv	–	–	–	–	–	–	–	–	–	–
Gravity	Various years	i	yes	yes	no	yes	yes	yes	yes	yes	yes	–
		ii	5.6	6.8	10	–	22.2	21.5	24.45	22.2	21.5	24.45
		iii	0.43	0.43	1.5	–	4.5	4.5	4.5	4.5	4.5	–
		iv	–	–	–	–	–	–	–	–	–	–
Seismic reflection	2009-2010	i	no	no	no	no	yes	yes	yes	yes	yes	yes
		ii	–	–	–	–	22.5	21.5	25.45	22.2	21.5	24.45
		iii	–	–	–	–	4.5	4.5	4.5	4.5	4.5	4.5
		iv	–	–	–	–	–	–	–	–	–	–
Magnetotelluric	2010	i	no	no	no	no	yes	no	yes	yes	yes	yes
		ii	–	–	–	–	22.5	21.5	25.45	22.2	21.5	24.45
		iii	–	–	–	–	4.5	4.5	4.5	4.5	4.5	4.5
		iv	–	–	–	–	–	–	–	–	–	–

Explanations: (i) Was this profile measured using/coincide with the following geophysical method?, (ii) L= measured length [km], (iii) D = approximate interpretation depth in this study [km], (iv) A= area [km²].

Depending on each survey's aim and the desired investigation depth, different geophysical data were integrated for studying the shallow and deep-scale subsurface geology (Table 1). Although the majority of these geophysical data were previously interpreted and their joint or individual interpretation outlined several results which improved basic geological knowledge of the Skellefte district (Weihed 2015), a joint and multi-scale geophysical study which integrates all these previously acquired geophysical data was lacking. Therefore, we propose new models which are compatible with seismic, MT and potential field data. Moreover, in this study the magnetic and gravity model of Profile E-1 has been proposed to constrain previous interpretations of the resistivity/IP data.

The shallow-scale and deep-scale geophysical studies are classified based on the resolution and investigation depth of each method. Shallow investigations provide a high resolution image of the subsurface down to ~ 1.5 km depth and include 2D and 3D resistivity/IP data (Tavakoli *et al.* 2012a, 2016) constrained with potential field data. Deep investigations include seismic reflection (Dehghannejad *et al.* 2012a), MT (García Juanatey 2012) and potential field data (Tavakoli *et al.* 2012b) which provide a deep image of the subsurface down to ~ 4.5 km depth.

The potential field data have been modeled and interpreted together with resistivity and IP data in a local-scale along 2D profiles and in a 3D area. Tavakoli *et al.* (2012a) studied the effectiveness of the resistivity/IP method to detect the sulphide mineralization, or its alteration halo which was also constrained by magnetic and gravity modeling. The result proved promising, as several high chargeability zones were indicated, among which one with a known mineralization which was already proven by drilling. This was the motivation for deeper geoelectrical investigation thereby the subsurface resistivity down to ca. 1.5 km depth as well as inside a 3D area was imaged (Tavakoli *et al.* 2016). The result from new data strengthened some earlier interpretations, but also provided new insights about anomalies at greater depths (*i.e.*, 0.5–1 km depth). On the other hand, the 3D data, although cover a very small area compared to all other geophysical results, provided valuable result about the distribution of the sulphide ore around the Maurliden deposits (Tavakoli *et al.* 2016). Potential field data was also used to confirm, and in some cases improve the interpretation of the seismic reflection data (Tavakoli *et al.* 2012b). Among others, the TIB mafic intrusive rocks were imaged similarly on seismic reflection and potential field results, imaging the basal detachment zone at 3.5–4.5 km depth. The potential field data constrained the large-scale models in the areas where the seismic reflection sections were blank, or unable to provide information due to, *e.g.*, the verticality of the contacts. The MT data could particularly provide information about the deeper parts of the study area, *e.g.*, the ore related hydrothermally altered

metavolcanic rocks within the Skellefte Group are depicted as conductors and have been found at depths between 1 and 6 km in the CSD. Shallower occurrences are not detected or are masked by conductive shales from the Vargfors Group. Also, the Jörn intrusion reaches 6.2 km depth and is characterized by an inhomogeneous distribution of resistivity values (García Juanatey 2012).

Similar studies with diverse range of geophysical data have focused on applying a joint inversion in multi dimensions using different approaches (direct parameter coupling and cross-gradient coupling) in terms of physical parameters and their coupling, for which the results show improvement over single inversions (see, *e.g.*, Moorkamp *et al.* 2011). Represas *et al.* (2015) examines the joint inversion of the gravity and resistivity data and compares it with the individual inversion of each dataset, which indicates that the joint inversion, although more complicated and time consuming, provides more realistic and geologically meaningful models than the ones calculated by inversion of each data set individually. However, this study does not aim to apply the joint inversion due to dimensionality and confidentiality of the data; instead, a joint interpretation is motivated.

Although these geophysical studies revealed interesting results from different scales (varying from ~ 0.5 km down to 4.5 km), they have never been interpreted jointly, together with other collected data from same scale. In this study we aim to integrate these models in the two scales of local and regional and confirm, or otherwise propose new interpretations accordingly. The joint interpretation of the data can then: (i) improve the shallow and deep-scale models of the subsurface by suggesting new interpretations based on the integrated geophysical studies, and (ii) identify new areas to prospect the hosting structures for the sulphide mineralization as a guide for future exploration activities and drilling plans.

2. GEOLOGICAL BACKGROUND

The Skellefte district rocks (Fig. 1) comprise metamorphosed Palaeoproterozoic supracrustal and intrusive rocks that were deformed and metamorphosed (Kathol and Weihed 2005). The 1.9-1.89 Ga Skellefte Group rocks are dominated by subaqueous lava domes, porphyritic cryptodomes, lavas and volcanoclastic rocks with largely rhyolitic composition (Allen *et al.* 1996) and minor occurrences of basalts, andesites and dacites (Billström and Weihed 1996) which form the lowermost stratigraphic unit in the district. Sedimentary rocks of the Vargfors Group overlie the Skellefte Group and form a distinct sub-basin, the Vargfors basin, in the northern part of the central Skellefte district. The lowermost parts of the Vargfors Group stratigraphy comprise turbiditic mudstones and sandstones overlain by monomict con-

glomerates, whereas the upper parts of the Vargfors stratigraphy are limited to the Vargfors basin and are characterized by polymict conglomerates formed in alluvial fans and braided river systems (Bauer *et al.* 2011, 2013). Metasedimentary rocks to the south of the central Skellefte district are regarded as rocks of the Vargfors Group due to their similar character and lithology. Their transition to Bothnian Supergroup metasedimentary rocks to the south of the district has been arbitrary (Kathol and Weihed 2005). The upper parts of Vargfors stratigraphy are dated at 1875 ± 4 Ma from an intercalated ignimbrite (Billström and Weihed 1996). The oldest intrusive rocks in the Skellefte district are represented by 1.89–1.87 Ga Jörn-type early orogenic intrusive rocks (Fig. 1). The central Skellefte district is characterized by a complex fault pattern of NNW-SSE-striking normal faults and associated NE-SW-striking transfer faults formed during crustal extension (Fig. 1; Bauer *et al.* 2011). The earliest tectonic deformation at 1.89–1.87 Ga is constrained to deeper crustal levels and formed synchronously with upper crustal extension and Skellefte Group volcanism (Skyttä *et al.* 2012). Subsequent SSW-NNE crustal shortening at 1.87 Ga resulted in reactivation of the NNW-SSE syn-extensional faults with S-side-up shearing (Bauer *et al.* 2011) and upper crustal coaxial deformation with steep to sub-vertical mineral lineations (Skyttä *et al.* 2012). The latest major deformation event at 1.82–1.80 Ga (Weihed *et al.* 2002) results from E-W crustal shortening causing reactivation and accompanied reverse shearing along steeply-dipping N-S-striking high-strain zones (Bergman and Weihed 2001).

Allen *et al.* (1996) argues that VMS deposits in the Skellefte district could have been formed as sub-seafloor replacement within volcanoclastic sediments in the uppermost parts of the Skellefte Group stratigraphy. Previous studies suggested that the ore-forming hydrothermal fluids utilised the syn-extensional faults as fluid conduits and the ores precipitated in the vicinity of these faults (Allen *et al.* 1996, Bauer *et al.* 2013).

3. GEOPHYSICAL DATA

Seismic reflection, MT and potential field data have been used for deep-scale imaging of the subsurface (~ 4.5 km depth), and resistivity/IP data contributed to model a high resolution image of the geological structures within the shallower parts (*i.e.*, down to ~ 1.5 km). Most of interpretations were constrained by physical properties of the rocks, including magnetic susceptibility (μ), density, resistivity, and chargeability from both outcrop samples, and drill-cores (Tavakoli *et al.* 2012a). A brief description of the geophysical data including field surveys and interpretations are explained in this chapter. Information regarding each specific geophysical method, profile length and investigation depths is summarized in Table 1.

3.1 Resistivity and IP data

During two field campaigns, resistivity and chargeability of the subsurface was measured along three profiles (I, II, and E-1; Tavakoli *et al.* 2012a, 2016) and inside an area in 3D (Tavakoli *et al.* 2016). The field work was carried out using pole-dipole electrode configuration; however, each survey was designed using a specific electrode array and hence different penetration depths were acquired. The pole-dipole electrode array was preferred since the array is sensitive to horizontal variation of the resistivity at depth and according to Nyquist and Roth (2005) has higher signal strength compared to dipole-dipole array. In addition, its lower EM coupling compared to Wenner array and higher penetration depth compared to dipole-dipole makes this array favorite for this study.

2009-resistivity/IP Profiles I and II

In 2009, a geoelectrical campaign was initiated to delineate and model the geometry of the shallow subsurface, down to ~ 430 m (profiles I and II; Tavakoli *et al.* 2012a). The field work was carried out using pole-dipole electrode array; it consisted of five potential electrodes located 200, and 400 m apart. Profile I was extended over 6.8 km and positioned sub-parallel to the 5.6 km long profile II, covering a total length of 12.4 km around the Vargfors basin (Fig. 2). Further description of the field work and data processing is given by Tavakoli *et al.* (2012a).

2010-resistivity/IP Profile E-1

Profile E-1 was measured in 2010 to provide a deeper resistivity/IP image of the subsurface compared to the 2009 profiles (Fig. 2). In contrary to the 2009 profiles for which the potential dipoles (px-py) possessed a constant spacing of 200 m from the current electrode C1, in 2010 C1 was moved between a group of fixed dipoles which were connected differently, depending on the distance of the dipole to C1 (Tavakoli *et al.* 2016). Profile E-1 was 10 km long, covered the SW continuation of Profile II, and imaged the top 1.5 km of the upper crust. Since the field survey was conducted in a forward and reverse manner, the asymmetrical pattern of the data which is often produced when using pole-dipole array is reduced. Further details regarding the field survey and data processing are explained by Tavakoli *et al.* (2016).

2010-3D-resistivity/IP data

The resistivity/IP data were also measured in 3D (Fig. 2), covering a ~2.16 km² area of interpretation in the CSD (Tavakoli *et al.* 2016). The main purpose of the 3D resistivity/IP measurement was to better understand the 3D distribution of the sulphide mineralizations in the vicinity of Maurliden-North, East and Central mineralization and to investigate the possibility of

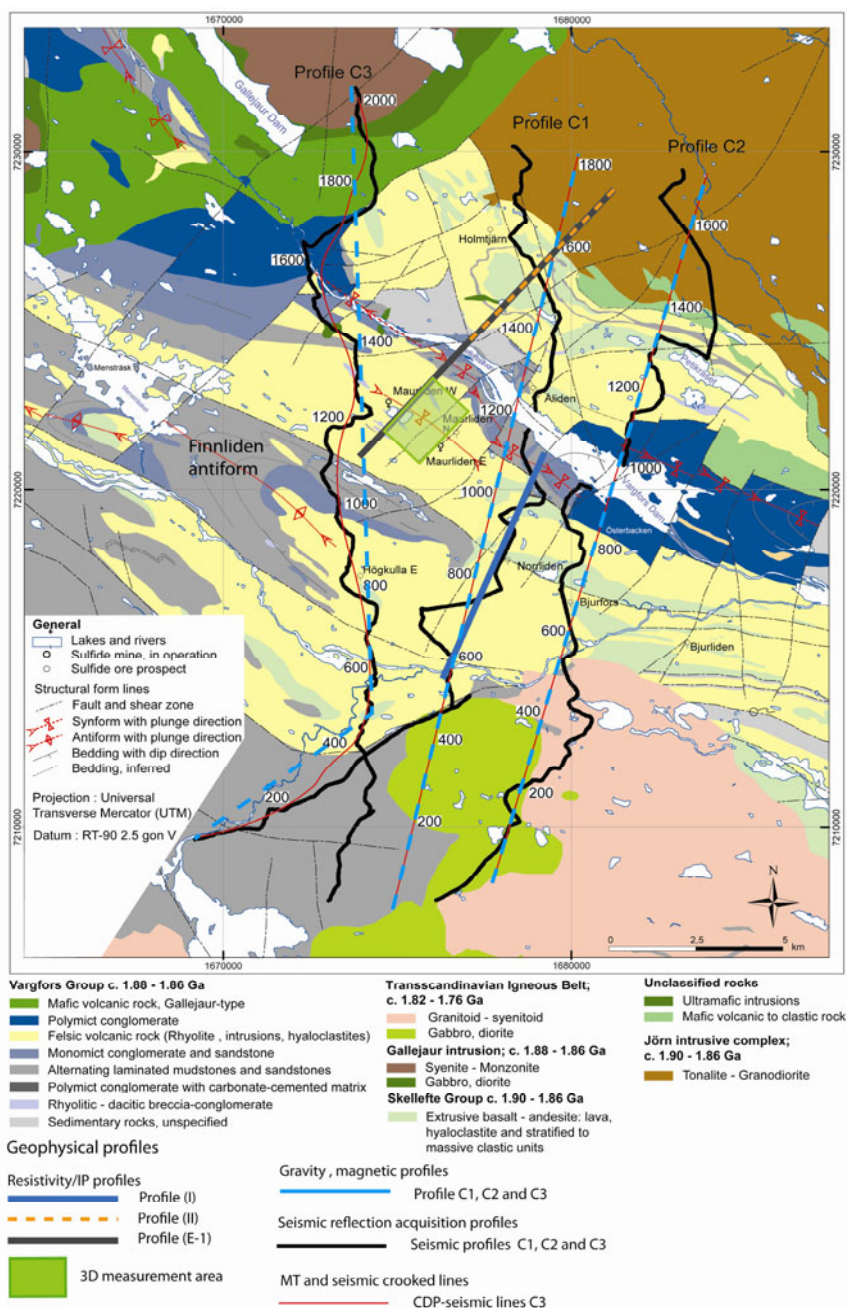


Fig. 2. Geophysical profiles; profiles I, II, E-1 and 3D-area for shallow-scale investigations and profiles C1, C2 and C3 for deep-investigations (modified after Bauer 2010).

detecting new geological features related to the sulphide mineralization. The result imaged the resistivity/chargeability distribution of the top ~450 m of the crust. Further details about the 3D-survey are explained by Tavakoli *et al.* (2016).

3.2 Magnetic and gravity data

Magnetic and gravity data were compiled from a database of SGU and Boliden mineral AB. The magnetic data consisted of a network with 40 m station spacing, whereas the spacing between gravity data varied between 200 and 800 m (Tavakoli *et al.* 2012a). In the sparsely distributed gravity areas along resistivity/IP profiles, additional gravity data were measured by Boliden Mineral AB in 2010, to increase the data density in the vicinity of the profiles. The IGRF correction was applied to the magnetic data with the total field intensity of 52612, inclination 76.7, and declination 6.7 (Model Vision Pro™, Encom Technology). However, the data in the modeled sections are presented in the original form. In addition, all necessary corrections, *i.e.*, latitude, drift, tidal, free air, instrument height, and Bouguer plate have been applied on the gravity data.

The magnetic and gravity modeling was performed on all geophysical profiles in this study (profiles I, II, E-1, C1, C2, and C3) in different scales: (i) shallow 2009-resistivity/IP profiles I and II down to 430 m depth, (ii) 2010-resistivity/IP Profile (E-1) down to 1.5 km, and finally (iii) reflection seismic and MT profiles C1, C2, and C3 down to 4.5 km depth. Potential field modeling of the geophysical profiles was carried out using Model Vision Pro™ (Encom Technology) in 2.5D, where the geological bodies are assumed to have a variable length in their strike direction. Further details about the potential field modeling and their processing procedure are explained by Tavakoli *et al.* (2012a, b).

3.3 Seismic reflection data

During 2009-2010, three sub-parallel and ~N-S trending seismic reflection profiles were acquired (profiles C1, C2, and C3; Fig. 2) to constrain a 3D geological model of the study area (see, Dehghannejad *et al.* 2012a). Each profile was about 30 km long and located approximately 3-7 km apart from the neighboring profile. The profiles were placed perpendicular to the main structural grain of the central Skellefte district. A SERCEL 408UL recording system from the Department of Earth Sciences, Uppsala University, was used for the data acquisition. A hydraulic hammer, VIBSIST, was used to generate the seismic signal and enabled imaging the subsurface structures down to ~4.5 km depth. The vehicle-mounted hammer hit the ground repeatedly at an increasing rate for a predetermined time span (Juhlin *et al.* 2010,

Dehghannejad *et al.* 2010, Malehmir *et al.* 2011). The geophones had a natural frequency of 28 Hz. In total, about 3000 shot points were generated along the three profiles with a nominal number of 2-4 sweeps per shot point, depending on the ground condition. Shot spacing was 25 m except in a few places where regular shot spacing was not possible due to a lack of road accessibility. Receiver spacing was 25 m with a large gap where Profiles C1 and C2 cross the Skellefte River. Processing work mainly followed conventional approaches in crystalline environment and experiences obtained from crooked-line data processing in the western part of the Skellefte district (Dehghannejad *et al.* 2010, 2012b). Further details about the seismic data acquisition, processing and results are explained by Dehghannejad *et al.* (2012a).

3.4 MT data

In fall 2010, 34 broadband MT sites were installed in the central Skellefte District, nearby the Mauriliden mine. The sites had 1-2 km spacing along two profiles in the NNE-SSW direction with ~23 km length and 3 to 4 km in between. The five MT channels, four for the horizontal electric and magnetic fields and one for the vertical magnetic field, were recorded. The data processing and estimation of the MT transfer functions, was carried out with the algorithm MTU2000 of Smirnov (2003). The obtained transfer functions were in the range of 700 Hz to 200 s, showing a decrease in apparent resistivities, with increasing periods, from 10 000 to 200 Ωm , while phases increase from 40° to 80°. Further details about the acquisition, processing, inversion and interpretation of the data are explained by García Juanatey (2012).

4. RESULTS

In this part, a summary of the geophysical investigations in different scales is presented. The integrated interpretation of the shallow-scale and deep-scale models were then presented and discussed in the discussion parts which includes new interpretations as well as supports to some of the earlier model results.

4.1 Shallow investigations (2D, 3D resistivity/IP and potential field data)

Shallow investigations include interpretation for profiles I, II, E-1 and the 3D-measurement area. In addition to profiles I and II which were modeled with magnetic and gravity data (Tavakoli *et al.* 2012a), the gravity and magnetic response of Profile E-1 is also modeled and presented. The 3D-area partly coincides with Profile E-1 and has a too small surface coverage to be modeled with magnetic and gravity data; hence they have not been modeled

with potential field data. The inversion of the resistivity profiles was carried out using Res2Dinv (Loke 2012) with least-square method. The resistivity and chargeability models did not indicate any irregular variation in the values in lower sections. Therefore, we used the default depth weighting factor of 1.05 to compensate for the resolution loss at greater depths. We also allowed the program to determine the depth weighting factor automatically which the resulting section was similar to when 1.05 was used. The effects of the side blocks were also slightly diminished to decrease the effect of artefacts in the inversion result.

Profiles I and II

Basic information about the subsurface geometry of Profile I was acquired from resistivity/IP investigations (Fig. 3a). A study of the resistivity and

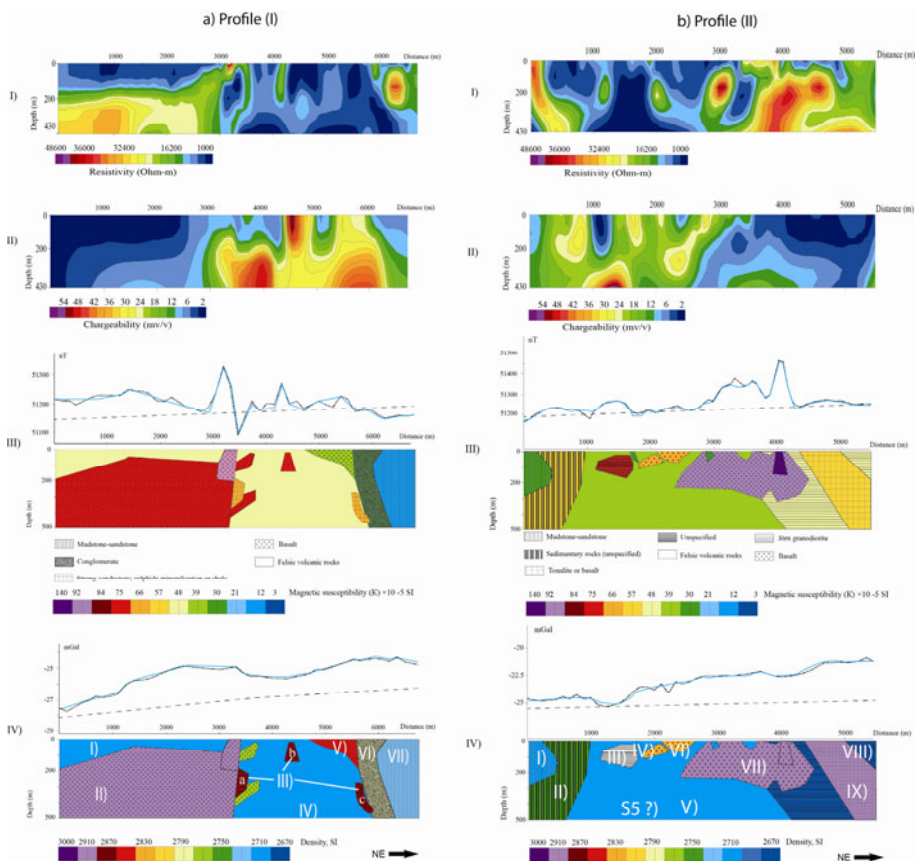


Fig. 3. RIMD models of profiles I and II; (a) Profiles I: (i) resistivity, (ii) IP, (iii) magnetic, (iv) gravity; (b) Profile II: (i) resistivity, (ii) IP, (iii) magnetic, (iv) gravity.

chargeability of the massive sulphide samples from Norrleden-N deposit indicated a zone with high chargeability and high conductivity (Tavakoli *et al.* 2012a). The resistivity/IP result from Profile I imaged three zones (a, b, and c; Fig. 3a-IV). Tavakoli *et al.* (2012a) explain these anomalies as new potential prospects for sulphide mineralization or graphitic schist. The resulted resistivity/IP data was further modeled using potential field data (Figs. 3a-III and 3a-IV). The RIMD (resistivity, IP, magnetic, density) model delineated the geometry of Profile I down to 430 m depth (Fig. 3a). Profile (II) was measured sub-parallel to Profile I and cut through the contact between the Vargfors-Skellefte Group and Skellefte-Jörn units (Tavakoli *et al.* 2012a). The synclinal structure of the Vargfors basin was indicated on both resistivity and IP data, where the inter-sedimentary contact of the Vargfors basin was imaged as a result of a resistivity contrast between the sandstone and unspecified sedimentary rocks (contact I-II; Fig. 3b). In addition, the NE-dipping contact between the Skellefte Group rocks and the Jörn intrusion is indicated on final (RIMD) (contact V-VIII; Fig. 3b). An outstanding high IP anomaly at $\sim x = 1300$ m (body S5; Fig. 3b-IV) was identified within the deeper parts of the Skellefte Group felsic volcanic rocks and therefore interpreted as a likely structure related to the alteration zones which might envelope the sulphide mineralization or graphitic schist. However, since the high IP anomaly was located at the bottommost part of the depth section, additional investigations are required for any further interpretations.

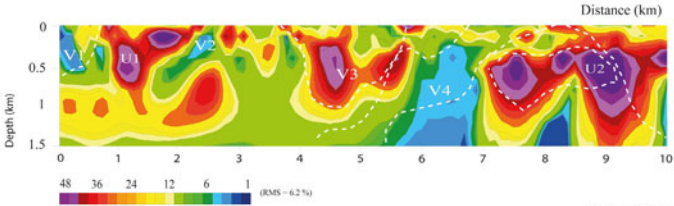
Profile E-1

Profile E-1 is a horizontal extension of Profile II to the SW (Fig. 2), and in comparison to Profile II, images the subsurface down to a greater depth (~ 1.5 km). Several IP anomalies were identified in the inversion result of Profile (E-1) which are mainly associated with low resistivities (S1-S5 in Fig. 4a and b; Tavakoli *et al.* 2016). The high chargeability anomaly labeled S5 in Profile II is associated with S4 and S5 in Profile E-1 which implies that the high IP signature in Profile II was not an artifact, but a possible indication of a conductive structure related to the sulphide mineralization or a graphitic schist (Tavakoli *et al.* 2016). Another IP anomaly interpreted as a graphitic schist (V4; Fig. 4b) which dips to the SW, together with S5 appear in the vicinity of the Skellefte-Vargfors Group contact in the north, and thus are the most likely features related to the alteration zones around sulphide mineralization in Profile E-1 which are enveloped by V4 (Fig. 4a and b; Tavakoli *et al.* 2016).

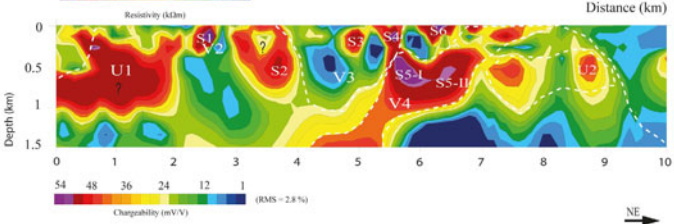
3D-measurement area

Result from interpretation of the 3D resistivity/IP data includes eight depth sections, starting from 50 m in depth down to ~ 450 m (Fig. 5). A part of the

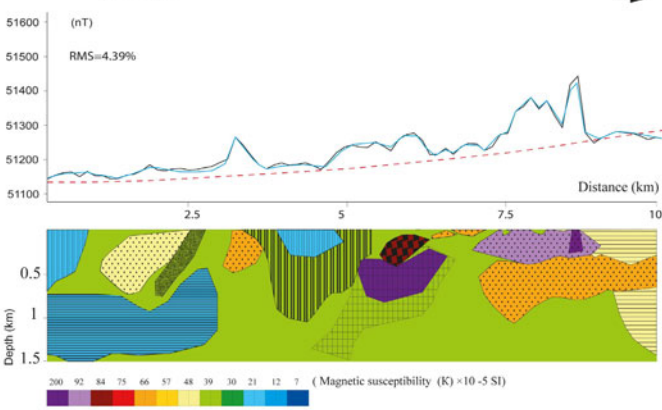
a) Resistivity model



b) IP model



c) Magnetic modelling



d) Gravity modelling

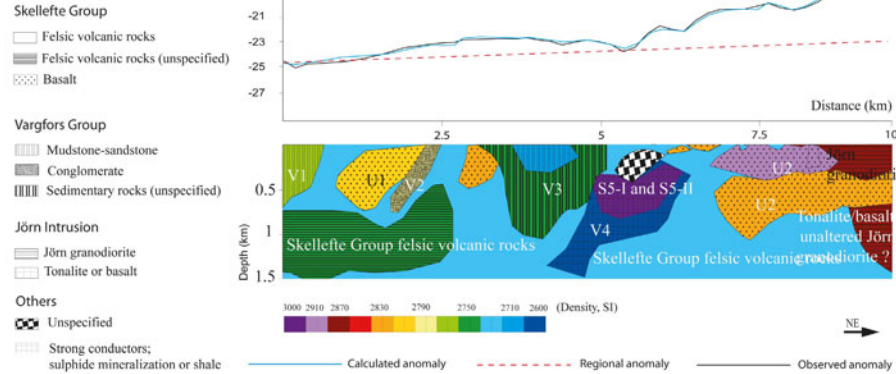


Fig. 4. Integrated geophysical modeling along Profile E-1: (a) resistivity model, (b) IP model, (c) magnetic model, (d) gravity model.

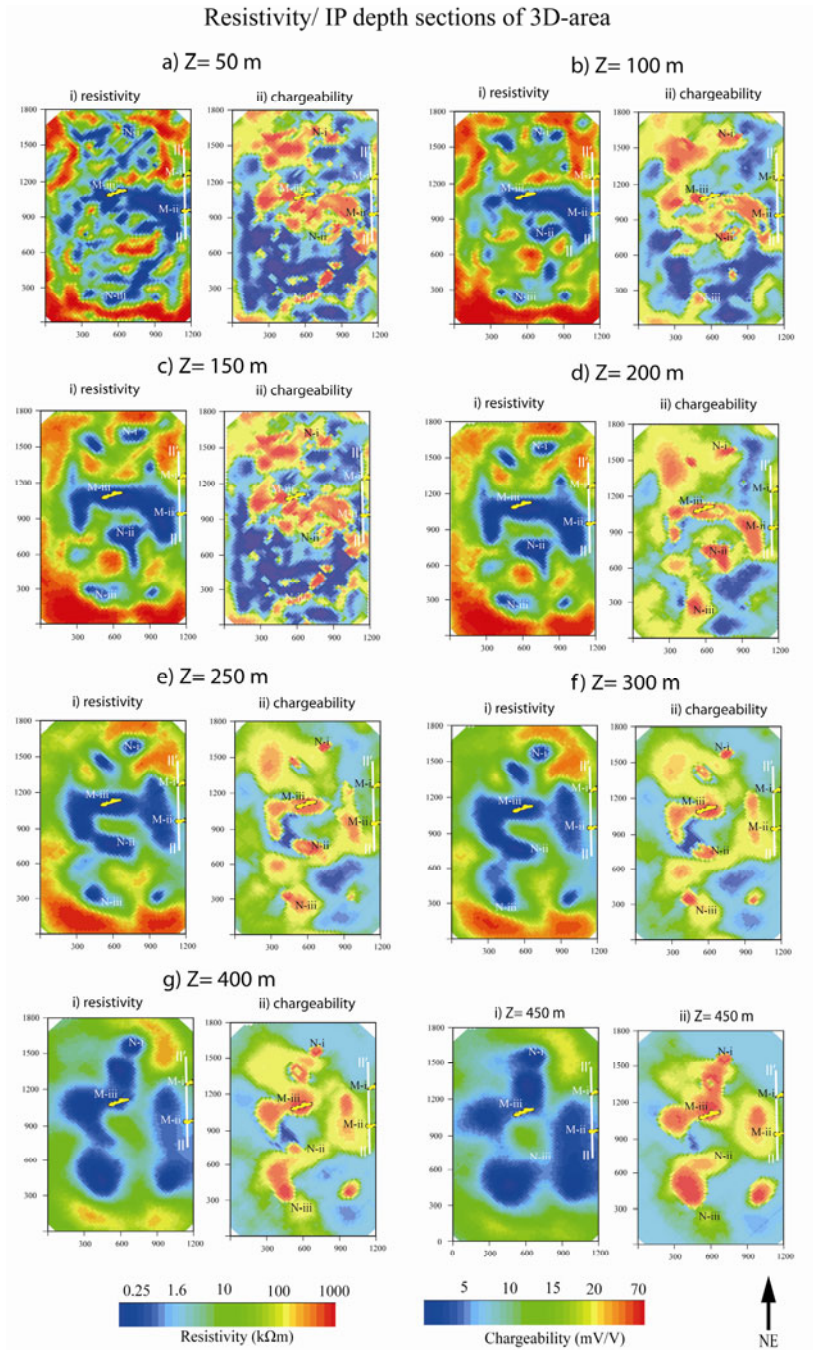


Fig. 5. Resistivity and IP depth sections of the 3D-area for shallow interpretations down to 450 m depth.

3D-area coincides with the profile II-II' of Montelius *et al.* (2007) which studied the distribution of the sulphide mineral related to the Maurliden (North, East and Central) domain.

A Central Conductive Zone (CCZ) which coincides with the Maurliden-East and Central mineralization was identified on both resistivity and IP data from 3D-area. The conductivities are within the range of $\sim 1 \text{ k}\Omega\text{m}$ and have chargeability ranged between 20 and 70 mV/V, which is within the range of measured chargeability for the VMS deposits (Tavakoli *et al.* 2012a). The unusually high resistivity of the Maurliden-North deposit ($\sim 50 \text{ k}\Omega\text{m}$) is related to the unaltered structure of the hosting felsic volcanic rocks or low concentration, or disseminated pattern of the VMS deposits (Tavakoli *et al.* 2016). Anomaly M-iii shows the greatest depth extent among the three studied Maurliden mineralizations (Fig. 5). In addition to the Maurliden mineralizations, three new conductive zones were detected inside the 3D-area which may be related to the structures hosting sulphide mineralization (Fig. 5; Tavakoli *et al.* 2016).

4.2 Deep investigations (seismic reflection, potential field, and MT data)

Preliminary interpretation of the seismic profiles C1, C2, and C3 (Fig. 2) was conducted by Dehghannejad *et al.* (2012a). Several reflectors were explained as major faults and shear-zones and were related to lithological contacts (Dehghannejad *et al.* 2012a). The magnetic, and gravity response of the three seismic profiles were calculated down to $\sim 5 \text{ km}$ in depth to verify or otherwise improve the seismic interpretations (Tavakoli *et al.* 2012b). In addition, the resistivity of the subsurface structures in profiles C1, C2, and C3 has been estimated through inversion of the 3D MT data (García Juanatey 2012).

Seismic reflection data

Seismic reflection data along Profile C1 reveals that the southernmost part of this profile is more reflective than the central and the northern part (Fig. 7a). A series of south-dipping reflections, each with slightly different dip angle, extend to the surface and were interpreted to depict a series of major shear zones (Dehghannejad *et al.* 2012a). The northern parts of Profile C1 are dominated by shorter reflections which are related to the southern contact of the Jörn intrusive complex.

In contrast to the results observed along Profile C1, the central part of C2 is more reflective than its southern part. A synformal structure extending to a $\sim 1.7 \text{ km}$ depth corresponded to the Vargfors basin (R8 and R15 in Fig. 6b; see also Bauer 2010). In addition, several weak reflections observed in the northern part of the profile C2 were interpreted to originate from the southern contact of the Jörn intrusive suite (Dehghannejad *et al.* 2012a). A series

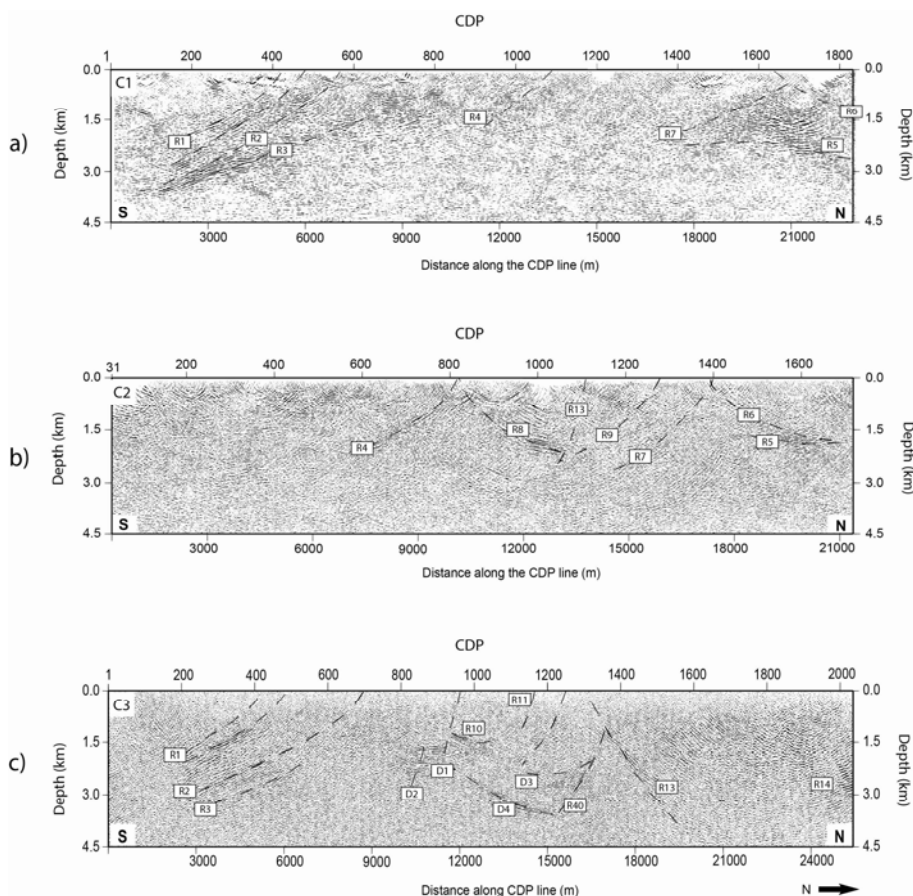


Fig. 6. Migrated seismic section of the seismic reflection profiles along the CDP lines in the central Skellefte district: (a) Profile C1, (b) Profile C2, and (c) Profile C3. Vertical: horizontal (scale) = 90% for a, b, and c. Modified after Dehghannejad *et al.* (2012a).

of south-dipping reflections are observed in the southern part of the Profile C3, similar to the south-dipping reflections identified on Profile C1 (Fig. 7c). These reflections show similar character in both profiles, suggesting identical geological structures (Dehghannejad *et al.* 2012a). The diffractions, as well as some reflections, are segmented by a set of south-dipping shear zones, sub-parallel to other reflections (Dehghannejad *et al.* 2012a).

Potential field modeling

The magnetic and gravity modeling along Profile C1 suggest that among south-dipping reflectors (R1, R2, and R3) in profiles C1 and C3, only R2 co-

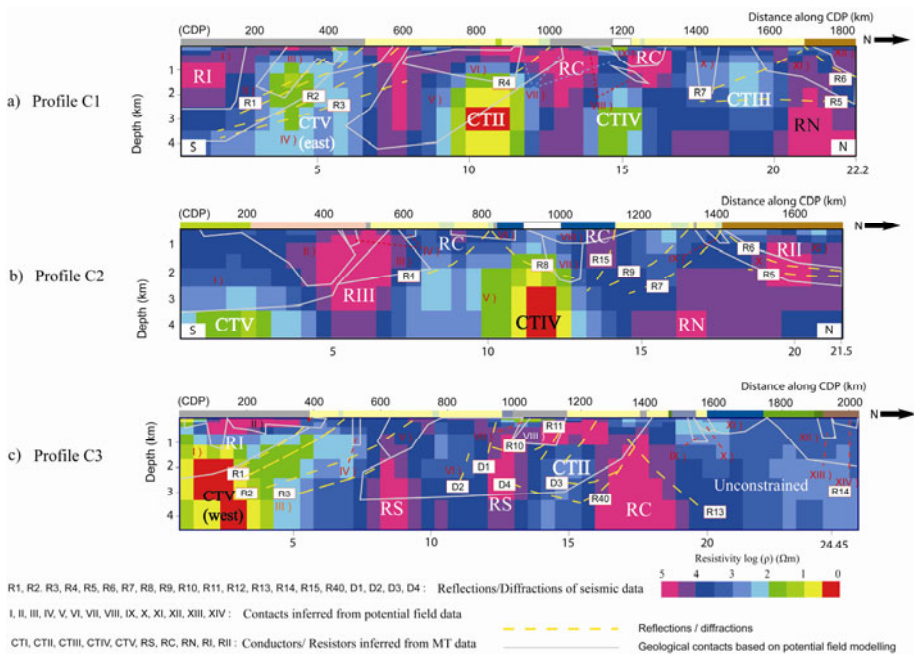


Fig. 7. Integrated deep-investigations along profiles C1, C2, and C3 using seismic reflection (Dehghannejad *et al.* 2012a), potential field data (Tavakoli *et al.* 2012b), and MT data (García Juanatey 2012).

incides with the model inferred from interpretation of the potential field data (Fig. 7). In addition, in the north, reflectors R6 and R7 support the result from magnetic and gravity modeling which delineates the NE-dipping contact between the Jörn intrusion and its underlying rocks (contact XI-XII; Fig. 7a) as well as the contact between the deep basalt and Skellefte Group felsic volcanic rocks (contact IV-X in Fig. 7a; Tavakoli *et al.* 2012b).

Modeling of the magnetic and gravity data greatly contributed to the interpretation of the southern part of Profile C2, since no reflector was observed within the 7 km beginning of this profile (Fig. 7b). Thus, the spatial relationship between lithologies in this part (TIB Gabbro, Skellefte Group, and Vargfors Group rocks) is only delineated and explained by the result of magnetic and gravity data. Further to the north, reflectors R4, R6, and R8 coincide with the models acquired from interpretation of the magnetic and gravity data (Tavakoli *et al.* 2012b).

Geometry of the key geological structures along Profile C3 was well delineated in areas where the seismic reflections/diffraction coincided with the result from magnetic and gravity modeling (R1, R3, R11, R4, and D3; Fig. 6c). Potential field data, however, did not provide an insight on subdivi-

sion of the blocks indicated by diffractions D1, D2, and reflection R10, since their surrounding lithology indicates similar petrophysical signatures; this is also due to the large station spacing for the gravity data (Tavakoli *et al.* 2012a).

MT models

The sliced depth sections of the 3D MT data in this study were integrated for interpretation along CDP lines of the profiles C1, C2, and C3. However, in order to compare MT interpretation with the result from seismic and potential field data, deep investigation in this study is limited down to 4.5 km depth.

Prominent and deep sub-vertical conductors at the fringe of the model (*e.g.*, CTV; Fig. 7b) are possibly related to the crustal-scale shear zones that surround the study area. Additionally, several conductors at intermediate depths (between 1–4 km depth) are associated to hydrothermally altered rocks within the ore bearing Skellefte Group (*e.g.*, CTII, CTIII, and CTIV; Fig. 6a and b). These conductors occur at the intersections of near-vertical transfer faults inferred from field observations (Bauer *et al.* 2011), normal listric faults interpreted from seismics (Dehghannejad *et al.* 2012a), and possible vertical faults imaged by the 3D MT model. In addition, several high resistivity structures were identified within upper parts of the models, supporting interpretation of the potential field data (Tavakoli *et al.* 2012b), which relates these anomalies to shallow basalts (*e.g.*, II, IV, V; Fig. 7c).

5. DISCUSSION

5.1 Shallow interpretations down to 1.5 km depth

This section summarizes new conclusions from joint interpretation of profiles I, II, E-1 and a 3D-area based on the resistivity/IP and potential field data. The top 1.5 km of the MT data were also taken into account for possible correlation. The key interpretations inferred from modeling of profiles I, (II), and (E-1) and 3D data are described below:

(i) Resistivity and chargeability data for body II (Fig. 3a–IV) which was interpreted as Skellefte Group basalt agrees with MT interpretation indicating similar high resistivity response on MT and resistivity sections (at CDP 600–900; Fig. 8a).

(ii) The NE-dipping geometry of the Vargors-Skellefte contact in its southern part is consistent in profiles E-1 and I (IV–VI in Profile I and AF–V3 in Profile E-1; Fig. 7). However, understanding the depth to the deeper parts of the Vargfors basin along Profile (I) was not possible due to the limited investigation depth. Yet, Profile (E-1) shows that this part of basin is ex-

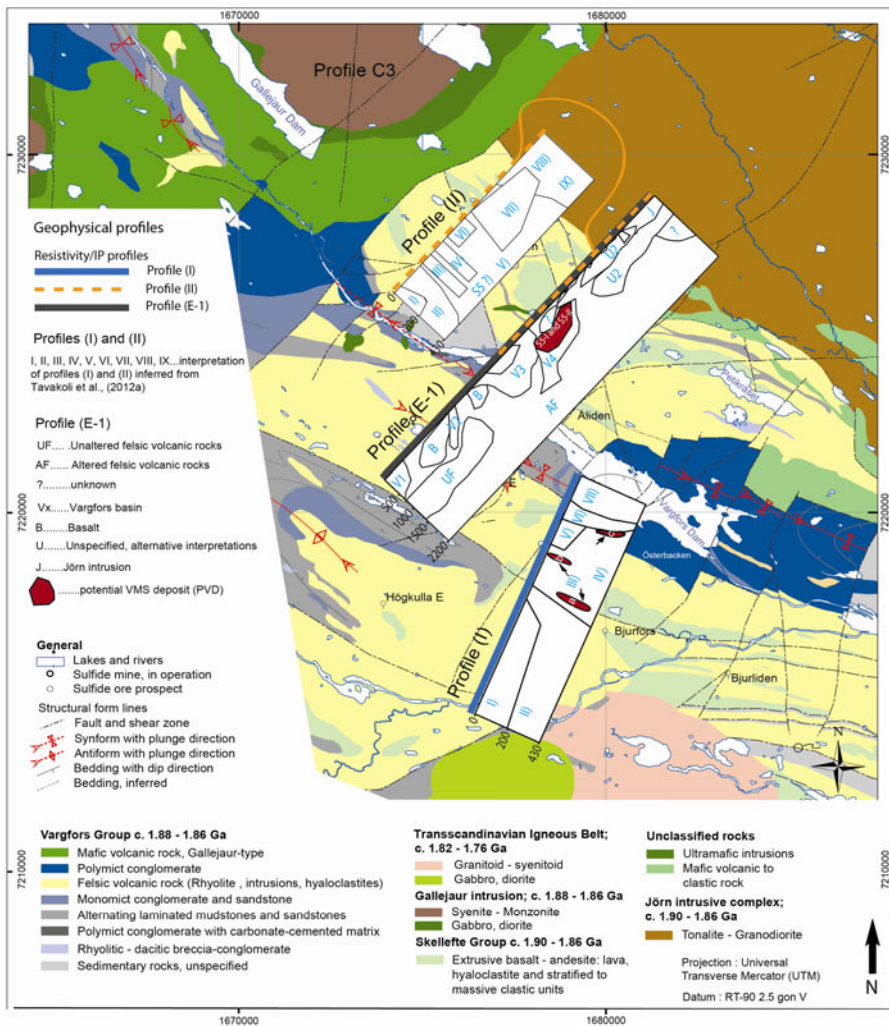


Fig. 8. 2D-shallow profiles and their interpretations inferred from resistivity, IP and potential field data; depth sections have been exaggerated vertically (modified after Bauer 2010).

tended at depth down to a maximum of ~ 1 km, but the maximum depth of the basin is probably more than this.

(iii) A high chargeability body (S5 in Profile II; Fig. 7) which was observed in Profile II in the study by Tavakoli *et al.* (2012a) is probably an indication of structures related to the sulphide mineralization (S5-I and S5-II in Profile E-1; Fig. 7) which implies that S5 is very likely to denote sulphide mineralization and is enveloped by a conductive material such as graphitic

schist. This interpretation agrees well with a result from potential field modeling along Profile E-1 where the sink in the gravity anomaly coincides with low density graphitic schist (body V4; Fig. 8) and underlies the Vargfors basin close to the contact with the felsic volcanic rocks (Tavakoli *et al.* 2016). The conductive zone labeled S5 and its enveloping graphitic schist is also identified in the MT data along Profile C1 between 0.5 and 2.5 km depth (CTIII at CDP 1400-1600 in profile C1; Fig. 7a).

(iv) The geometry of the Vargfors basin in profile (E-1) is consistent with the resistivity, IP and magnetic interpretations (Fig. 4a-c). Also, its synformal structure, suggested by Bauer (2010), agrees well with the joint interpretation along the studied profiles I, II, and E-1. However, the unusual gravity high for the basin along 2D-profiles (Figs. 3a-IV, 3b-IV, and 4d) probably resulted from large scale and deep structures at greater depths, or low resolution of the gravity data due to large station spacing.

(v) New potential field modeling along Profile (E-1) reveals that the Jörn intrusion is underlain by unaltered granodiorites, with minor occurrences of basalts, which compensate the gravity high within the northernmost end of Profile E-1. This interpretation is in agreement with pervious resistivity/IP, potential field, seismic and MT studies (reflector R6, resistor RN; Fig. 8a and b) (Dehghannejad *et al.* 2012a, García Juanatey 2012, Tavakoli *et al.* 2012a, b, 2016).

(vi) New result from potential field modeling along Profile E-1 indicates that almost all anomalies labeled S, which were explained as potential features related to the sulphide mineralizations, are associated with magnetic highs. In addition, the SE part of Profile E-1 is associated with magnetic and gravity lows, which is in agreement with the dominant lithology inferred from interpretation of the geophysical data (Fig. 4).

The conductive zones inside the 3D-area imaged the known Mauriliden (North, East, and Central) mineralizations (Mi, M-ii, and M-iii; Fig. 5) as well as new zones (N-i, N-ii, and N-iii; Fig. 5) which provide new possibilities for detecting structures related to mineralization. A comparison between the resistivity/chargeability result from 2D and 3D data reveals that S1 can depict the Mauriliden mineralization (Figs. 4b and 5). Due to a rather limited depth extent of the 3D-area (~ 450 m), and since the deep profiles C1, C2 or C3 do not coincide with, or pass nearby the 3D-area, seismic reflection or MT, or potential field data are unable to contribute to constrain this interpretation. The top-left corner of the 3D area indicates an interesting anomaly on the chargeability model sections which continues from near surface down to 400 m at depth. S1 could therefore be a projection of this anomaly on Profile E-1, which makes this anomaly an interesting feature related to the VMS mineralization.

5.2 Deep interpretations down to 4.5 km depth

The joint interpretation of the potential field, seismic reflection and MT data along three sub-parallel profiles C1, C2, and C3 was conducted to delineate a deep image of the CSD and new models were proposed. As a result, the earlier magnetic and gravity models have undergone minor modifications to fit the MT, seismic and potential field data simultaneously. The modified models (Fig. 7) are indicated with brown lines in the depth sections (Fig. 9). Seismic reflection data have been used for VMS exploration in other studies and have proven successful. Exceptions are, *e.g.*, short and shallow reflectors that cross-cut through the main lithological contacts which may be difficult to provide explanation for all such reflections (Bellefleur *et al.* 2015). Hedin *et al.* (2013) in an integrated geophysical study in central Sweden conducted 3D interpretation of the subsurface structures in the vicinity of boreholes based on seismic reflection and bedrock geology data, which result was constrained by 3D inversion of the gravity data. The integrative interpretation resulted in better control on the structures of interest for the scientific deep

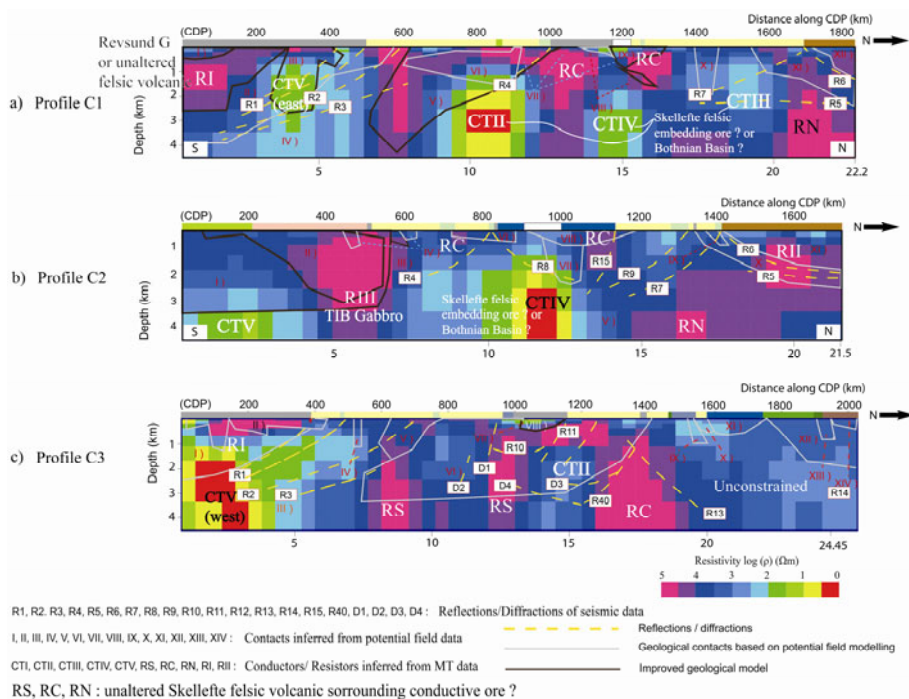


Fig. 9. Improved deep-scale model acquired inferred from seismic reflection, potential field data and MT data. Geometry of the several geological bodies has been modified based on MT interpretations.

drilling project. Hübner *et al.* (2013) used magnetotelluric data to construct 3D resistivity model of the upper crust along the previously collected seismic profiles in Kristineberg area, northern Sweden. The study utilized integration of seismic reflection data into the interpretation that demonstrated good correlation between the reflectors and main electrical features along the MT profiles and provided support to some of the earlier interpretations based on the seismic data, but also proposed new interpretations.

Profile C1

The laminated sandstone-mudstone (body I; Fig. 7a) in the SW end of profiles C1 and C3, demonstrates an unusual high resistivity (100 k Ω m) on MT data along Profile C1, which is well above the expected resistivity (\sim 4200 Ω m) of the Vargfors sandstone-mudstone based on the study by Tavakoli *et al.* (2012a). Although the seismic data could not image the contact between body I and the surrounding rocks, MT data nicely corresponds to the geometry of the sandstone-mudstone inferred from potential field interpretation (body I; Fig. 7a).

The deep conductor, CTV (east) coincides with bodies II, III, and IV in profile C1. Reflector R2 was coincided and interpreted as a contact between TIB Gabbro and felsic volcanic rocks based on potential field-seismic interpretation (Fig. 7a). However, García Juanatey (2012) relates the deep conductor CTV (east) to either (i) an alteration zone which implies that the Skellefte volcanic rocks are dipping and extending further to the south, or (ii) a near surface signature of the crustal detachment explained by Skyttä *et al.* (2012). However, according to the potential field interpretations (Tavakoli *et al.* 2012b), and given the fact that body II indicates an inconsistent internal structure (density and magnetic susceptibility variations), we suggest that the western part of body II (at $x = 3$ –4 km; Fig. 9a) is attributed to the TIB Gabbro, with high resistivity, density and magnetic susceptibility. Conductor CTIV, with \sim 10–100 Ω m resistivity is explained as an alteration zone embedding the sulphide mineralization (García Juanatey 2012), and therefore supports the interpretation inferred from potential field data, which explains bodies V and IV as two different felsic volcanic rocks (Fig. 9a). Therefore, reflector R4 represents the contact within the felsic volcanic rocks of the Skellefte Group (R4 and contact V-IV; Fig. 9a).

Although bodies VIII, IX, and X do not coincide completely with the MT data (Fig. 7a), they reveal new interpretation which improves the result of potential field modeling. Interestingly, the vicinity of the northern resistor RC to the surface in Profile C1 can signify that body IX, representing the Vargfors basin, has probably a shallower depth extent (\sim 0.8 km) compared to the one (\sim 1 km) inferred from potential field data (Tavakoli *et al.* 2012b) and has its maximum depth in its SW (compare IX in Figs. 7a and 9a). Con-

ductor CTIII, which was interpreted as alteration zone within the Skellefte Group felsic volcanic rocks, is in agreement with the model based on potential field data, as body V4 was interpreted to be a similar feature in the study by Tavakoli *et al.* (2012b) (see CTIII in Fig. 9a and V4 in Fig. 8).

García Juanatey (2012) relates the resistor RN to the basaltic break-back faults which coincide with reflector R5. The faulted contact along the NE parts of Profile C1 (contact XI-XII; Fig. 9a) fits well to the potential field, seismic reflection and MT data. This is indicated by reflector R6 which images the faulted contact between bodies XI and XII (Fig. 9a).

Profile C2

The southern contact of body I fits nicely with resistivity variation near conductor CTV (10-1000 Ωm ; Fig. 9b), which García Juanatey (2012) relates to either an alteration zone, or conductive faults associated with graphite/sulphide. García Juanatey (2012) relates resistor RIII to the TIB type granitoid-syenitoid which partly fits to the model suggested based on interpretation of the potential field data and explains body II as TIB granitoid-syenitoid (Fig. 7b). The geometry of the bodies I and II was therefore slightly modified to make a better fit with both MT and potential field models (Fig. 9b). Due to the lack of seismic reflectors, the seismic data cannot verify or reject this interpretation.

García Juanatey (2012) relates the deep conductor CTIV to either altered felsic volcanic rocks which embed the ore or graphite within the fault. Conductor CTIV in Profile C2 coincides with a part of body V (at CDP 750-1000), and its upper parts are bounded by resistor RC (interpreted as unaltered felsic volcanic rocks) and reflectors R15 and R8, which are interpreted as fault controlled reflectors (Dehghannejad *et al.* 2012a). However, the considerably low resistivity of CTIV between 2.5 and 5 km depth (Fig. 9b) is somewhat too low to explain even strongly altered felsic volcanic rocks, and CTIV is too large to be related to the hosting rocks of the sulphide mineralization. Hence we suggest that CTIV probably images the sedimentary rocks of the Bothnian Basin with high content of graphite, which is regarded as a basement for hydrothermally altered felsic volcanic rocks of the Skellefte Group (Weihed *et al.* 2002, Skyttä *et al.* 2012).

Geometry of the Vargfors basin (body VIII; Fig. 7b) could not be constrained or modeled either with MT or with the seismic reflection data. However, the resistivities ranging from 1 000 Ωm (CDP 950; Fig. 9b) to 10 000 Ωm (CDP 110; Fig. 9b) support the model suggested by Tavakoli *et al.* (2012b). Resistor RII in the NE, fits nicely with the model indicating contact X-XI which depicts the boundary between the Skellefte group basalt and the Jörn granodiorite inferred from potential field interpretations (Tavakoli *et al.* 2012b) and seismic reflection data (reflector R6; Dehghannejad *et al.*

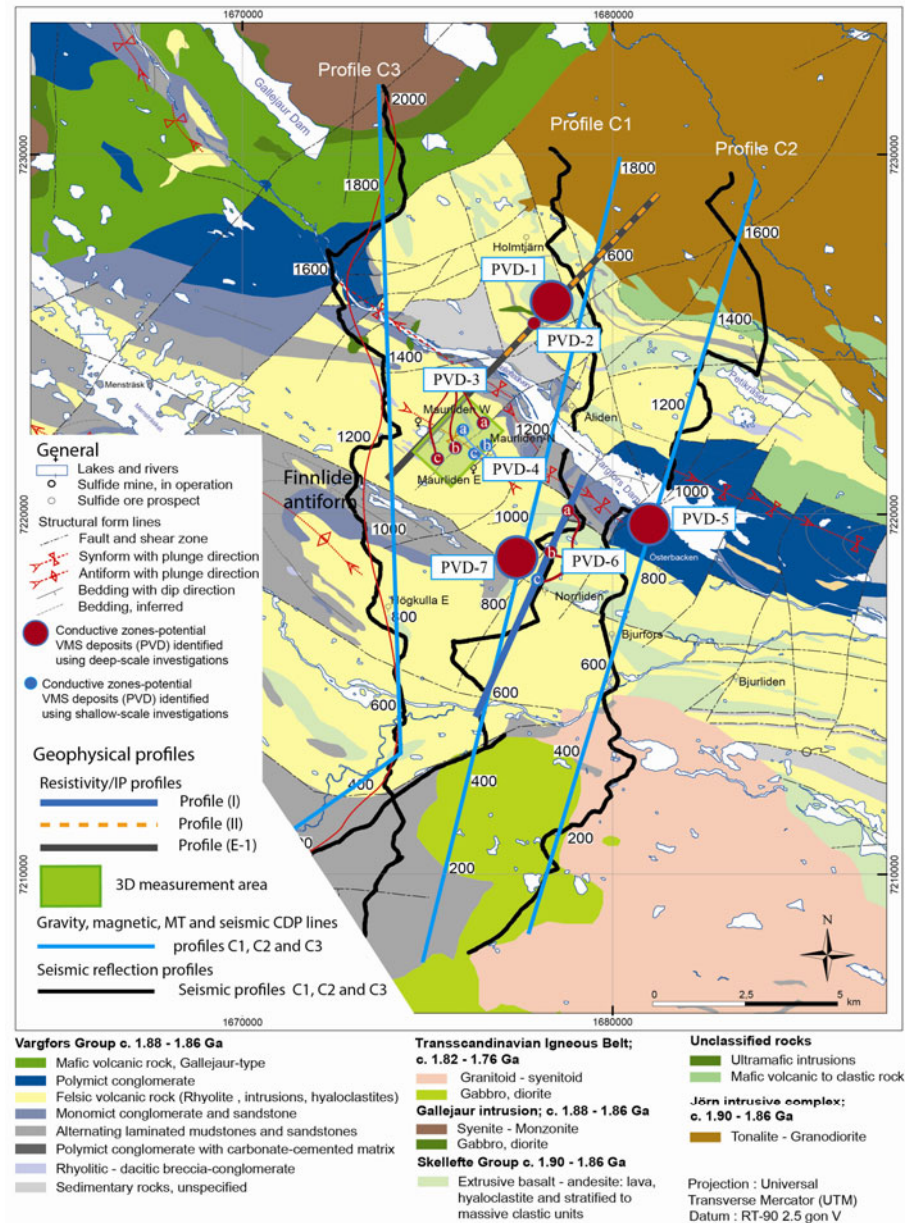


Fig. 10. Distribution of the conductive zones/PVD zones inferred from shallow and deep-scale investigations of the geophysical data in the CSD (modified after Bauer 2010).

2012a). This interpretation is also consistent with the result of deep resistivity/IP investigation for the neighboring Profile E-1, where a resistivity similar to that of RII is observed for the Jörn intrusion and its underlying basalt/unaltered granodiorite (see X-XI in Figs. 9b and 4).

Profile C3

Reflector R1 which Dehghannejad *et al.* (2012a) explained as a product of inverted normal fault, and which isolates the sandstone-mudstone and their underlying rocks (Tavakoli *et al.* 2012b), terminates before reaching the conductive zone CTV west (Fig. 7c). Hence CTV west either images the faults within the laminated sandstone or the shear zone (DNSZ; Fig. 1). Frequent intercalation of the highly magnetized basalts along the laminated sandstone-mudstone was previously explained by Tavakoli *et al.* (2012b) which agrees well with the high resistivity of these basalts inferred from MT interpretation (*e.g.*, body II; Fig. 9c). In addition to the shallow basalts, bodies IV and V, interpreted as deep and sub-vertical basaltic structures, coincide with the high resistivity zone (10 000 Ωm) observed on MT data (at CDP 500-800; Fig. 9c). Unspecified felsic volcanic rocks along Profile C3 (VI; Fig. 9c) which indicate a lower degree of alteration than rhyolites, are bounded with reflectors R3 and R40 and diffraction D3 (Tavakoli *et al.* 2012b). Reflector R11 fits well with the contact VIII-VI which bounds the eastern side of Vargfors basin.

The NE parts of Profile C3 (CDPs 1750-2000) is associated with the TIB-type Gabbro (XIII) and syenite-monzonite (XIV) belonging to the Gallejaure intrusion, which overly the deeply extended Skellefte Group basalts (XII). While this part of Profile C3 is seismically transparent, these intrusive rocks were modeled with the potential field data (Tavakoli *et al.* 2012b). Although XIII and XIV are probably too small to be modeled with MT interpretation, MT result imaged the XII-III boundary (Fig. 9c) which coincides with a group of gently north-dipping reflectors (R14; Dehghannejad *et al.* 2012a).

Several sites were identified as features related to the potential VMS deposits (PVD) based on integrated geophysical and geological interpretations in near-surface and deep-scales. Although these zones were identified based on the modeling of the different datasets, and hence have different certainty, they have great potential for prospecting sulphide mineralization (Fig. 10).

6. CONCLUSION

Multiple geophysical data including magnetic, gravity, resistivity, IP, MT and seismic reflection data were integrated in the central Skellefte district to confirm or improve previous interpretations. The main aim of this study was

thus to understand the key lithological features in the two scales of shallow, *i.e.*, down to 1.5 km and deep, *i.e.*, down to 4.5 km in depth.

The result from near-surface investigations confirms that the sulphide mineralization often occurs within the lowermost contact of the Vargfors basin and uppermost part of the Skellefte Group felsic volcanic rocks. The joint interpretation of the 2D-profiles I, II, and E-1 have benefited from potential field modeling along Profile E-1, which adds new insights about the geometry of the area around the Vargfors basin. Several key lithological contacts which were identified in previous studies, *e.g.*, the Jörn-Skellefte contact and the contact between the Skellefte Group-Vargfors Group, were validated in this study. In addition, the basaltic dykes which were inferred from resistivity/IP models fit nicely with the new magnetic model along Profile E-1. Almost all S IP anomalies which were explained as features related to the sulphide mineralization were associated with the magnetic highs which support earlier interpretation for Profile E-1. The deeper resistivity/IP image of Profile E-1 revealed that the anomaly observed on IP model of the Profile II is not an artifact and can depict sulphide mineralization.

Results from deep-investigations revealed new information from greater depths. Joint interpretation of the seismic reflection, potential field and MT data particularly helped to explain several enhanced conductive areas as well as high resistivity zones, which were not detected by seismic and potential field data. Majority of the shallow basalts coincided nicely with the high resistivities observed on MT data; however, some interpretations proved contradictory, which lead to modifying the earlier models and proposed a better model fit consistent with all three datasets. The enhanced conductivities inferred from MT data and confirmed by seismic and/or potential field data suggested new horizons for targeting the sulphide mineralization. The failure in detecting small-scale known mineralization with the MT data, which were detected using high resolution resistivity/IP studies, implies the significance of the multi-scale interpretations which can be determined depending on the aim and scope of studies. The near-surface and deep-scale models of the central Skellefte district are therefore of great importance for further exploration activities in the area. Seven zones with high probability of features related to the potential VMS deposits (PVD zones) were identified within the top 4 km of the crust. These zones, although initially identified based on resistivity, IP or MT data, correlate at least to another geophysical method, *i.e.*, seismic reflection and potential field data in deep-scale and potential field data in shallow-scale which makes these anomalies interesting zones for future focus of the exploration activities in the area.

Acknowledgement. This study is conducted as a part of the VINNOVA 4D modeling project and is financed by VINNOVA and Boliden

Mineral AB. All 4D-modeling members are thanked for their contribution, provision of data and their comments on this manuscript. We also thank Geovista AB for their contributions to the field work and data processing. The authors would like to thank editors of the *Acta Geophysica* journal and two anonymous reviewers for their constructive comments.

References

- Allen, R.L., P. Weihed, and S.-Å. Svenson (1996), Setting of Zn–Cu–Au–Ag massive 1256 sulfide deposits in the evolution and facies architecture of a 1.9 Ga marine volcanic 1257 arc, Skellefte District, Sweden, *Econ. Geol.* **91**, 6, 1022-1053, DOI: 10.2113/gsecongeo.91.6.1022.
- Bauer, T. (2010), Structural and sedimentological reconstruction of the inverted Vargfors Basin – A base for 4D-modelling, Licentiate Thesis, Luleå University of Technology, Sweden, 44 pp.
- Bauer, T.E., P. Skyttä, R.L. Allen, and P. Weihed (2011), Syn-extensional faulting controlling structural inversion – Insights from the Palaeoproterozoic Vargfors syncline, Skellefte mining district, Sweden, *Precambrian Res.* **191**, 3-4, 166-183, DOI: 10.1016/j.precamres.2011.09.014.
- Bauer, T., P. Skyttä, R. Allen, and P. Weihed (2013), Fault-controlled sedimentation in a progressively opening extensional basin: the Palaeoproterozoic Vargfors basin, Skellefte mining district, Sweden, *Int. J. Earth Sci.* **102**, 2, 385-400, DOI: 10.1007/s00531-012-0808-x.
- Bellefleur, G., E. Schetselaar, D. White, K. Miah, and P. Dueck (2015), 3D seismic imaging of the Lalor volcanogenic massive sulphide deposit, Manitoba, Canada, *Geophys. Prospect.* **63**, 4, 813-832, DOI: 10.1111/1365-2478.12236.
- Bergman Weihed, J. (2001), Palaeoproterozoic deformation zones in the Skellefte and Arvidsjaur areas, northern Sweden. In: P. Weihed (ed.), *Economic Geology Research*, Vol. 1, Geological Survey of Sweden, C 833, 46-68.
- Billström, K., and P. Weihed (1996), Age and provenance of host rocks and ores in the Paleoproterozoic Skellefte district, northern Sweden, *Econ. Geol.* **91**, 6, 1054-1072, DOI: 10.2113/gsecongeo.91.6.1054.
- Dehghannejad, M., C. Juhlin, A. Malehmir, P. Skyttä, and P. Weihed (2010), Reflection seismic imaging of the upper crust in the Kristineberg mining area, northern Sweden, *J. Appl. Geophys.* **71**, 4, 125-136, DOI: 10.1016/j.jappgeo.2010.06.002.
- Dehghannejad, M., T.E. Bauer, A. Malehmir, C. Juhlin, and P. Weihed (2012a), Crustal geometry of the central Skellefte district, northern Sweden – constraints from reflection seismic investigations, *Tectonophysics* **20**, 87-99, DOI: 10.1016/j.tecto.2011.12.021.

- Dehghannejad, M., A. Malehmir, C. Juhlin, and P. Skyttä (2012b), 3D constraints and finite difference modeling of massive sulfide deposits: The Kristineberg seismic lines revisited, northern Sweden, *Geophysics* **77**, 5, 69-79, DOI: 10.1190/geo2011-0466.1.
- García Juanatey, M.A. (2012), Seismics, 2D and 3D inversion of magnetotellurics : Jigsaw pieces in understanding the Skellefte Ore District, Ph.D. Thesis, Uppsala University, Uppsala, Sweden.
- Hedin, P., A. Malehmir, D.G. Gee, C. Juhlin, and D. Dyrelus (2013). 3D interpretation by integrating seismic and potential field data in the vicinity of the proposed COSC-1 drill site, central Swedish Caledonides, *Geol. Soc. London Spec. Pub.* **390**, 301-319, DOI: 10.1144/SP390.15.
- Hübert, J., M. García Juanatey, A. Malehmir, A. Tryggvason, and L. Pedersen (2013), The upper crustal 3-D resistivity structure of the Kristineberg area, Skellefte district, northern Sweden revealed by magnetotelluric data, *Geophys. J. Int.* **192**, 2, 500-513, DOI: 10.1093/gji/ggs044.
- Juhlin, C., M. Dehghannejad, B. Lund, A. Malehmir, and G. Pratt (2010), Reflection seismic imaging of the end-glacial Pärvie Fault system, northern Sweden, *J. Appl. Geophys.* **70**, 4, 307-316, DOI: 10.1016/j.jappgeo.2009.06.004.
- Kathol, B., and P. Weihed (eds.) (2005), *Description to Regional Geological and Geophysical Maps of the Skellefte District and Surrounding Areas*, Sveriges Geologiska Undersökning, Ser. Ba, 197 pp.
- Loke, M.H. (2012), Tutorial: 2-D and 3-D electrical imaging surveys, Geotomo Software, Malaysia.
- Malehmir, A., P. Dahlin, E. Lundberg, C. Juhlin, H. Sjöström, and K. Högdahl (2011), Reflection seismic investigations in the Dannemora area, central Sweden: insights into the geometry of poly-phase deformation zones and magnetite-skarn deposits, *J. Geophys. Res.* **116**, B11, B11307, DOI: 10.1029/2011JB008643.
- Montelius, C., R.L. Allen, S.-Å. Svenson, and P. Weihed (2007), Facies architecture of the Palaeoproterozoic VMS-bearing Maurliden volcanic centre, Skellefte district, Sweden, *GFF* **129**, 3, 177-196.
- Moorkamp, M., B. Heincke, M. Jegen, A.W. Roberts, and R.W. Hobbs (2011), A framework for 3-D joint inversion of MT, gravity and seismic refraction data, *Geophys. J. Int.* **184**, 1, 477-493, DOI: 10.1111/j.1365-246X.2010.04856.x.
- Nyquist, J.E., and M.J.S. Roth (2005), Improved 3D pole-dipole resistivity surveys using radial measurement pairs, *Geophys. Res. Lett.* **32**, 21, L21416, DOI: 10.1029/2005GL024153.
- Represas, P., F.A. Monteiro Santos, J.A. Ribeiro, A. Andrade Afonso, J. Ribeiro, M. Moreira, and L.A. Mendes-Victor (2015), On the applicability of joint inversion of gravity and resistivity data to the study of a tectonic sedimentary basin in Northern Portugal, *Pure Appl. Geophys.* **172**, 10, 2681-2699, DOI: 10.1007/s00024-014-0920-x.

- Skyttä, P. (2012), Crustal evolution of an ore district illustrated - 4D-animation from the Skellefte district, Sweden, *Comput. Geosci.* **48**, 157-161, DOI: 10.1016/j.cageo.2012.05.029.
- Skyttä, P., T.E. Bauer, S. Tavakoli, T. Hermansson, J. Andersson, and P. Weihed (2012), Pre-1.87 Ga development of crustal domains overprinted by 1.87 Ga transpression in the Palaeoproterozoic Skellefte District, Sweden, *Precambrian Res.* **206-207**, 109-136, DOI: 10.1016/j.precamres.2012.02.022.
- Smirnov, M. (2003), Magnetotelluric data processing with a robust statistical procedure having a high breakdown point, *Geophys. J. Int.* **152**, 1, 1-7, DOI: 10.1046/j.1365-246X.2003.01733.x.
- Tavakoli, S., S.-Å. Elming, and H. Thunehed (2012a), Geophysical modelling of the central Skellefte district, Northern Sweden; an integrated model based on the electrical, potential field and petrophysical data, *Appl. Geophys.* **82**, 84-100, DOI: 10.1016/j.jappgeo.2012.02.006.
- Tavakoli, S., T.E. Bauer, S.-Å. Elming, H. Thunehed, and P. Weihed (2012b), Regional-scale geometry of the central Skellefte district, northern Sweden-results from 2.5D potential field modeling along three previously acquired seismic profiles, *Appl. Geophys.* **85**, 43-58, DOI: 10.1016/j.jappgeo.2012.06.012.
- Tavakoli, S., T.E. Bauer, T.M. Rasmussen, P. Weihed, and S.-A. Elming (2016), Deep massive sulphide exploration using 2D and 3D geoelectrical and induced polarization data in Skellefte mining district, northern Sweden, *Geophys. Prospect.*, DOI: 10.1111/1365-2478.12363.
- Weihed, P. (2010), Palaeoproterozoic mineralized volcanic arc systems and tectonic evolution of the Fennoscandian shield: Skellefte district Sweden, *GFF* **132**, 1, 83-91.
- Weihed, P. (2015), *3D, 4D and Predictive Modelling of Major Mineral Belts in Europe*, Mineral Resource Reviews, Springer, 331 pp.
- Weihed, P., K. Billstrom, P. Persson, and J. Weihed (2002), Relationship between 1.90-1.85 Ga accretionary processes and 1.82-1.80 Ga oblique subduction at the Karelian craton margin, Fennoscandian Shield, *J. Geol. Soc. Sweden* **124**, 3, 163-180.

Received 21 August 2015

Received in revised form 23 November 2015

Accepted 27 January 2016